International Journal of Recent Technology and Engineering (IJRTE)
ISSN: 2277-3878, Volume-8 Issue-3, September 2019

Numerical Research of Hall Current Influence on MHD Convective "Flow in Presence" of Jeffrey Fluid, "Heat and Mass Transfer

Y. Sunita Rani

Abstract*: *The reason of this study is to find a numerical solutions of Jeffrey's compact, non-stressed, smooth, conductive, magnetic hall currents in the vertical optical direction in the occurrence of heat_flux, "heat"(h) & group transmit. The limited dissimilarity is solved to explain the "equations"(Eq). The effect of different constraints on "velocity"(V), "temperature"(temp) & concentration distributions was investigated at the boundary layer. Also, there is a computational discussion about the effect of relevant or important factors on the coefficients of skin_friction and the rate of h and "mass"(m) relocate according to the values of Nusselt and Sherwood information correspondingly. Great interconnection is achieved by using Perturbation and Finite difference techniques. Applications of magnetic materials, MHD generators and crude oil refinements have been found in this model.

*Keywords: **MHD; Free Convection; Hall Current; Jeffrey Fluid; Finite difference method;***

I. INTRODUCTION

The learning of "MHD" found to be applicable to rotational energy (MHD) generator and thermal conversion mechanism of nuclear spacecraft for new space systems. In a physically powerful attractive field, the transmission functionality of "ionized_gases" differs as of metals. The current in ionizing gas is typically formed by electron"s colliding through another rated or nonaligned element. Ionized gas flow is comparative toward the potential apply while the "electric field" is too feeble. Whatever the electrical conductivity unmistakably depends on the attractive field if there is an incredible electrical field. Accordingly, the electrical field's parallel conductivity is diminished. The flow in this manner lessens opposite to the electrical just as attractive fields in the way. The Hall sway (Cowling[1]) is named this marvel. The impact of hole flow on MHD flow consumes remained investigated through several examiners for the use of research on MHD generators also hole accelerators. Shows an significant part in describing the flow characteristics of fluid difficulties.

Manuscript published on 30 September 2019

*** Correspondence Author**

Y. Sunita Rani*, Professor in Mathematics Department of H & S, CMR Engineering College, Kandlakoya(V), Medchal(Dist.) Hyderabad, Telangana State, India. Phone No: 9966992400,Email Id: ysunitarani@gmail.com

Hole flow causes secondary fluid flow, which is correspondingly a characteristic of Coriolis strength. Hall effect in fluid flow is used in the production of various astrophysics and geophysics, as well as in the production of M.H.D, nuclear reactors as well as secretive energy storage. Therefore, it is recommended to study the joined effect of hole flow also cycle on the MHD fluid flow difficulties. Raju et al. [2] deliberate the present flow of M-H-D flanked by the included plates and the thin plates has been shown to favour Hall's c urrent effect.

II. LITERATURE SURVEY

Krishna and Reddy [3] studied the convection associated with the unstable MHD free-flow of the boundary moving through the medium. Prabhakar-Reddy also Anand-Rao [4] demonstrated the influence of radioactivity also heat on MHD free-standing channels passing through an infinite wall plate with Hall current and heat source. Rashad et al. [5] performed a study of a unique stationary tube located on a solid line with a vertical cylinder mounted in a non-Darcy Nano fluid-saturated filter. Rashidi_et_al. [6] investigated the examination of the 2nd rule of thermodynamics useful to an "electrically" conductive nano_fluid unsolidified graceful through an exposed circling capacitor between a solid outer surfaces. Watanabe and Pop [7] have shown the influence of Hall on an MHD borderline plate on a continuous plate. Sharma et al. [8] obtainable the results of Hall on an M/H/D varied tube with a non-viscous fluid that passed through a wall of molten oil, immersed in a high-speed/submerged flow. Sawaya et al. [9] proposed the Hall-scale test on behalf of electrolytic answers in a MHD flow symphonic system. Bhargava as well as Takhar [10] deliberate the guidance of Hall currents on the transfer of hydro magnetic warmth to viscoelastic fluid in a tube.

The investigation of Newtonian and non-Newtonian liquids is an extraordinary subject of premium. Researchers have been motivated by this region of research in view of the across the board utilization of Newtonian and non-Newtonian liquids in pharmaceutical, physiology, fiber innovation, nourishment items, covering wires, precious stone development, and so on. Maximum of the low-molecular heaviness affluences such as organic as well as non-organic solvents, resolutions for heavy molecular load mixtures also metal alloys exhibition stable Newtonian properties.

On behalf of this kind of solution/ingredient, the pressure of the cup is proportionate to the amount at which the shell is applied. Over the older few decades here has been an increasing appreciation of the fact that there are organisms of industrial consequence, particularly at different speeds (foam, emulsions, dispersion, suspension and distortion, etc.) also the polymeric melons as well as their explanations (together natural also synthetic) ensure not correspond to the Newtonian advance of the linear connection among hearing loss also the ratio of the series to a simple series. These liquids are known as non-Newtonian or nonlinear liquids. Non-Newtonian liquids are isolated into three particular gatherings: time-autonomous, free, viscoelastic and time-autonomous. In any case, actually, these classes are regularly not unmistakably characterized or obviously characterized. These liquids that display a blend of properties from the above gathering are depicted as unpredictable liquids, in spite of the fact that the term might be utilized in non-Newtonian liquid by and large. In such manner, there is no shared view for portraying Newtonian nonlinear conduct. Therefore, numerous models have been proposed in the writing to demonstrate non-Newtonian liquid sorts under various stream conditions. The most widely recognized and easiest model of a non-Newtonian viscoelastic liquid is Jeffrey liquid, which depicts the conduct of unwinding and unwinding.

The Jeffrey liquid model portrays the properties of a viscoelastic liquid, which is generally utilized in the polymer business. Maqbool et al. [11] considered the impact of rising divider tallness and divider thickness on a free sans mhd climate with Jeffrey liquid close to a level plate. vast packs set in as far as possible. Abbasi et al. [12] researched a liquid-filled container of Jeffrey liquid that isn't porous. Abbasi et al. [13] contemplated a two-dimensional laminar balance covered channel with a magneto hydrodynamic Jeffrey Nano fluid with blended convection. Khan [14] contemplated the progression of free MHD liquid moving through Jeffery liquid because of the moderate level plate that fulfills the divider qualities. Vajravelu_et_al. [15] exhibited the impact of free convection on the nonlinear vehicle of water through the Jeffrey garden in a divider mounted framework with a Brinkman model.

Lakshminarayana et al. [16] talked about the bearing of stream and warmth of peristaltic traffic in Jeffrey liquid in a hilter kilter cylinder mounted through the cylinder. The executive's likenesses are understood with annoyance strategies. Vajravelu et al. [17] detailed the progression of Jeffrey liquids into a vertical stratum with warmth move underneath the long hub and low Reynolds numbers. The peristaltic stream of Jeffrey liquid to the ventral cylinder is explored by Vajravelu et al. [18] utilizing blending methods. Jena et al. [19] found a warmth actuated impact of Jeffery's MHD liquid on the cylinder. Imtiaz_et_al. [20] found the impacts of homogenous & "homogenous" responses on Jeffrey M/H/D strains.

III. METHODOLOGY

Therefore, the purpose of this learning remained to spread Sharma as well as Chaudhary [21] to training the effects of Jeffrey fluid also angle of inclination . The equations governing the plate are modelled by a Cartesian coordinate system. Jeffrey's fluid model is presented mathematically and solved in a limited alteration method. Numerical solutions are offered on behalf of information on velocity, temperature, and deliberation profiles with variations of engineering parameters. This model includes important applications for industrial heat management, geological processes, MHD pumps, speeds and meters, geothermal storage and energy transport etc.

1. Formation of Flow Governing Equations :

The calculations of the motion of the viscous solid in the existence of the compelling field are:

Equation of continuity:

$$\nabla \cdot \bar{v} = 0 \tag{1}$$

Momentum Equation:

$$\rho\left[\frac{\partial \bar{v}}{\partial t} + (\bar{v}\cdot\nabla)\bar{v}\right] = -\nabla p + \bar{J}\times\bar{B} + \rho\bar{g} + \mu\nabla^2\bar{v} - \left[\frac{\mu}{k}\right]\bar{v} \tag{2}$$

Energy Equation:

$$\rho Cp\left[\frac{\partial T}{\partial t} + (\bar{v}\cdot\nabla)T\right] = k\nabla^2 T \tag{3}$$

Species Diffusion Equation:

$$\frac{\partial C}{\partial t} + (\bar{v}\cdot\nabla)C = D\nabla^2 C \tag{4}$$

Kirchhoff's first law:

$$\nabla \cdot \bar{J} = 0 \tag{5}$$

General Ohm's law:

$$\bar{J} + \frac{\omega_e \tau_e}{B_0}(\bar{J}\times\bar{B}) = \sigma\left(\bar{E} + \bar{v}\times\bar{B} + \frac{1}{e\eta_e}\nabla P_e\right) \tag{6}$$

Gauss's law of magnetism:

$$\bar{\nabla}\cdot\bar{B} = 0 \tag{7}$$

Introducing an "coordinate" scheme "(x', y', z')" through x' _axis "vertically" up_wards, y' _ axis usual to the plate_concentrating hooked on the liquefied area also z' _axis beside the thickness of the "plate". Let " $\vec{v} = u\hat{i} + v\hat{j} + w\hat{k}$ " remain the velocity, "$\vec{J} = J_x\hat{i} + J_y\hat{j} + J_z\hat{k}$" stay the present density at the argument "$p(x', y', z', t')$" as well as "$\bar{B} = \bar{B}_0\hat{J}$" be the applied magnetic field, '$\hat{i}, \hat{j}, \hat{k}$' being element vectors beside x' _axis, y' _axis as well as z' _axis correspondingly. Subsequently the plate is of in_finite length in "x' also z'" ways, consequently entirely the quantities excluding conceivably the weight are "independent of x' and z'". Currently, the eqn/(1) provides

"$\frac{\partial \bar{v}}{\partial y'} = 0$"

(8)

"Which is slightly fulfilled by"

$$\bar{v} = -V_0 \tag{9}$$

Where "V_0" is a constant and $V_0 > 0$. Consequently the velocity_vector_ $\bar{V}$ is assumed by

$$\bar{v} = u\hat{i} - V_0\hat{j} + w\hat{k} \tag{10}$$

"Again" the eqn/:(7) is fulfilled by

$$\bar{B} = \bar{B}_0\hat{j} \tag{11}$$

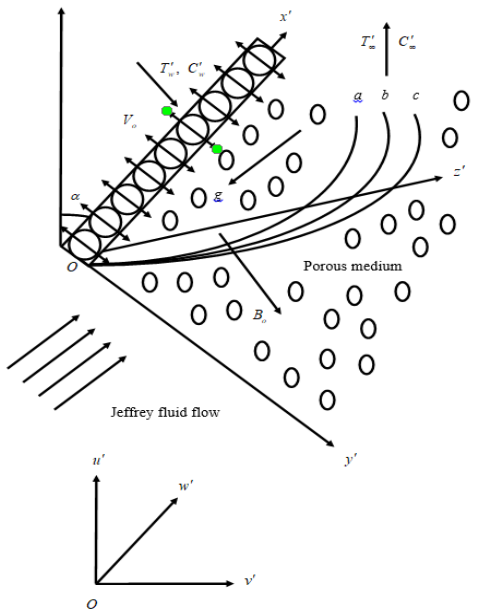

a --- "Momentum/boundary/layer", *b* --- "Thermal/boundary/layer", *c* --- "Concentration/boundary layer"

Fig. 1. Geometry/of the problematic

Likewise the eqn/(5) decreases to

$$\frac{\partial J_y}{\partial y'} = 0 \tag{12}$$

Which demonstrations that $J_y =$ constant. Meanwhile the plate is non/conducting, $J_y = 0$ at the plate also therefore $J_y = 0$ at totally points in the fluid. Therefore the present density is assumed by

$$\bar{J} = J_x\hat{i} + J_z\hat{k} \quad \text{----- (13)}$$

Under the assumption p_e, Electron pressure is continuous and $\bar{E} = 0$, the electric/field is zero then the equation/(6) proceeds the method

$$\bar{J} + \frac{m}{B_0}\left(\bar{J} \times \bar{B}\right) = \sigma\left(\bar{v} \times \bar{B}\right) \tag{14}$$

Wherever " $m = \varpi_e \tau_e$ " is the Hall_parameter? The equation--/(10),_(11)_(13), also_(14)_yield,

$$J_x = \frac{\sigma B_0}{1+m^2}(mu - w) \;\&\; J_z = \frac{\sigma B_0}{1+m^2}(u + mw)\Big\}$$

Hall currents, heat, and mass transfer occur when considering, compressing, viscous and conductive fluids flowing through the transient magneto hydrodynamic limit layer of the vertical tendency plate. The physical coordinates of the difficult are presented in Fig. 1. For this survey, the *x'*_axis is occupied with the slot as the source, with the plate leaning vertically in the way of the motion, also the *y'*-axis is perpendicular to the plate in the direction of ambient temperature T'_∞ as well as attentiveness C'_∞. A constant magnetic_field B_o is imposed along *y'*-axis and the effect of Hall currents is taken into explanation. The temp also the species attentiveness are continued at a suggested constant values T'_w and C'_w at the plate. Except for the buoyancy effect, it is expected that all the properties of the fluid are constant. We besides take on induction is the magnetic field is insignificant through respect to the applied magnetic field. This hypothesis is reasonable only if the magnetic Reynolds digit is very minor. The Cauchy pressure tensor, $\bar{S}$ of a "Jeffrey's" non_Newtonian fluid [29] proceeds the method as follows

$$\bar{S} = \frac{\mu}{1+\lambda}\left(\dot{\lambda} + \lambda_1\ddot{\lambda}\right) \tag{16}$$

Wherever μ is the forceful "viscosity", " λ_1 " is the RATIO of recreation to "retardation" times, dot overhead a amount signifies the substantial T "derivative" also λ is the shear_rate. The "Jeffrey_model" offers an elegant formulation that simulates the belongings of delay and relaxation that happen in non-Newtonian polymer flows. The cutting rate also the cutting velocity gradient are definite in more detail according to the velocity vector, $\bar{V}$, as follows:

$$\text{where } \dot{\lambda} = \nabla\bar{V} + (\nabla\bar{V})^T \tag{17}$$

$$\text{and } \ddot{\lambda} = \frac{d}{dt}\left(\dot{\lambda}\right) + (\bar{V}.\nabla)\dot{\lambda} \tag{18}$$

Equation of Continuity:

$$\frac{\partial v'}{\partial y'} = 0 \tag{19}$$

Momentum Equations:

$$\frac{\partial u'}{\partial t'} + v'\frac{\partial u'}{\partial y'} = \nu\left(\frac{1}{1+\lambda}\right)\frac{\partial^2 u'}{\partial y'^2} - \frac{\sigma B_0^2(u' + mw')}{\rho(1+m^2)} + g\beta(T' - T'_\infty)(\cos\alpha) + g\beta^*(C' - C'_\infty)(\cos\alpha) - \frac{\nu u'}{K'} \tag{20}$$

$$\frac{\partial w'}{\partial t'} + v'\frac{\partial w'}{\partial y'} = \nu\left(\frac{1}{1+\lambda}\right)\frac{\partial^2 w'}{\partial y'^2} + \frac{\sigma B_0^2(mu' - w')}{\rho(1+m^2)} - \frac{\nu w'}{K'} \tag{21}$$

Energy/Equation:

$$\frac{\partial T'}{\partial t'} + v'\frac{\partial T'}{\partial y'} = \frac{\kappa}{\rho C_p}\frac{\partial^2 T'}{\partial y'^2} \tag{22}$$

Species Diffusion Equation:

$$\frac{\partial C'}{\partial t'}+v'\frac{\partial C'}{\partial y'}=D\frac{\partial^2 C'}{\partial y'^2} \qquad (23)$$

Subject to the boundary situations

$$\left.\begin{aligned} t'\le 0: &\{u'(y',t')=0, w'(y',t')=0, T'(y',t')=0, C'(y',t')=0 \ \text{for all } y'\\ t'>0: &\begin{cases} u'(y',t')=0, w'(y',t')=0, T'(y',t')=ae^{\omega t'}, C'(y',t')=be^{\omega t'} \ \text{at } y'=0\\ u'(y',t')=0, w'(y',t')=0, T'(y',t')=0, C'(y',t')=0 \ \text{as } y'\to\infty \end{cases}\end{aligned}\right\} \qquad (24)$$

For the purpose of standardizing the flow model as well as facilitating numerical answers, the author must create the governing equations/(20), (21), (22) and (23) dimensionless under parameters (24) through implementing the previous dimensional quantities:

$$\left.\begin{aligned} &u=\frac{u'}{V_o}, y=\frac{y'V_o}{\nu}, t=\frac{t'V_o^2}{4\nu}, w=\frac{w'}{V_o}, \theta=\frac{T'-T'_\infty}{T'_w-T'_\infty}, \phi=\frac{C'-C'_\infty}{C'_w-C'_\infty}, K=\frac{K'V_o^2}{4\nu^2}, M=\frac{4\sigma\beta_o^2}{\rho V_o^2}, \omega=\frac{4\Omega}{V_0^2},\\ &\Pr=\frac{\rho\nu C_p}{\kappa}, Gr=\frac{4\nu g\beta(T'_w-T'_\infty)}{V_o^3}, Gc=\frac{4\nu g\beta(C'_w-C'_\infty)}{V_o^3}, Sc=\frac{\nu}{D}\end{aligned}\right\} \qquad (25)$$

parameters are described. The preceding non-dimensional forms are transformed by equations (20), (21), (22) as well as (23).

$$\frac{\partial u}{\partial t}-4\frac{\partial u}{\partial y}=4\left(\frac{1}{1+\lambda}\right)\frac{\partial^2 u}{\partial y^2}-\frac{M}{(1+m^2)}(u+mw)+Gr(\cos\alpha)\theta+Gc(\cos\alpha)\phi-\frac{u}{K} \qquad (26)$$

$$\frac{\partial w}{\partial t}-4\frac{\partial w}{\partial y}=4\left(1+\frac{1}{\gamma}\right)\frac{\partial^2 w}{\partial y^2}-\frac{M}{(1+m^2)}(w-mu)-\frac{w}{K} \qquad (27)$$

$$\frac{\partial\theta}{\partial t}-4\frac{\partial\theta}{\partial y}=\frac{4}{\Pr}\frac{\partial^2\theta}{\partial y^2} \qquad (28)$$

$$\frac{\partial\phi}{\partial t}-4\frac{\partial\phi}{\partial y}=\frac{4}{Sc}\frac{\partial^2\phi}{\partial y^2} \qquad (29)$$

The conforming borderline circumstances (24) non-dimensional forms are

$$\left.\begin{aligned} &t\le 0: \quad u=0, w=0, \theta=0, \phi=0 \ \text{for all } y\\ &t>0: \begin{cases} u=0, w=0, \theta=e^{i\omega t}, \phi=e^{i\omega t} \ \text{at } y=0\\ u=0, w=0, \theta=0, \phi=0 \quad \text{as } y\to\infty \end{cases}\end{aligned}\right\} \qquad (30)$$

The skin-friction at the plate, which is the non-dimensional form is assumed by

$$Cf_1=\left(\frac{1}{1+\lambda}\right)\frac{\left(\frac{\partial u'}{\partial y'}\right)_{y'=0}}{\rho V_o v}=\left(\frac{1}{1+\lambda}\right)\left(\frac{\partial u}{\partial y}\right)_{y=0} \text{ and } Cf_2=\left(\frac{1}{1+\lambda}\right)\frac{\left(\frac{\partial w'}{\partial y'}\right)_{y'=0}}{\rho V_o v}=\left(\frac{1}{1+\lambda}\right)\left(\frac{\partial w}{\partial y}\right)_{y=0} \qquad (31)$$

Cf_2 are Skin-friction coefficients alongside wall x' -axis as well as z' -axis respectively. The rate of heat transfer coefficient, which is the non_dimensional method in expressions of the "Nusselt_number" (*Nu*) is assumed by

$$Nu=-\frac{x'}{T'_w-T'_\infty}\left(\frac{\partial T'}{\partial y'}\right)_{y'=0} \Rightarrow Nu\,\mathrm{Re}_x^{-1}=-\left(\frac{\partial\theta}{\partial y}\right)_{y=0} \qquad (32)$$

The degree of form transmission coeff, which is the non_dimensional procedure in relations of the Sher_wood "number (*Sh*)", is assumed by

$$Sh=-\frac{x'}{C'_w-C'_\infty}\left(\frac{\partial C'}{\partial y'}\right)_{y'=0} \Rightarrow Sh\,\mathrm{Re}_x^{-1}=-\left(\frac{\partial\phi}{\partial y}\right)_{y=0} \quad \text{------ (33)}$$

where $\mathrm{Re}=\frac{V_o x'}{\nu}$ is the "local Reynolds_number".

1. **"Numerical_Solutions" By Finite Difference System :**

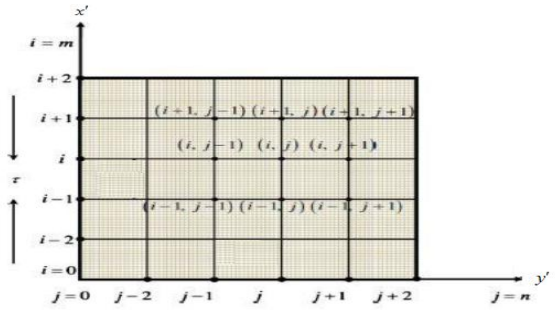

Fig. 2. Finite difference space grid

The non-straight force, vitality and fixation conditions are given in conditions (26), (27), (28) and (29) are fathomed under the suitable beginning and limit conditions (30) by the understood limited distinction strategy. The vehicle conditions (26), (27), (28) and (29) at the network point (I, j) are communicated in distinction structure utilizing Taylor's development:

$$\left(\frac{u_i^{j+1}-u_i^j}{\Delta t}\right)-4\left(\frac{u_{i+1}^j-u_i^j}{\Delta y}\right)=4\left(\frac{1}{1+\lambda}\right)\left(\frac{u_{i+1}^j-2u_i^j+u_{i-1}^j}{(\Delta y)^2}\right)-\frac{M}{(1+m^2)}\left(u_i^j+mw_i^j\right)$$
$$+(Gr)(\cos\alpha)\theta_i^j+(Gc)(\cos\alpha)\phi_i^j-\frac{u_i^j}{K}$$

-----(34)

$$\left(\frac{w_i^{j+1}-w_i^j}{\Delta t}\right)-4\left(\frac{w_{i+1}^j-w_i^j}{\Delta y}\right)=4\left(\frac{1}{1+\lambda}\right)\left(\frac{w_{i+1}^j-2w_i^j+w_{i-1}^j}{(\Delta y)^2}\right)-\frac{M}{(1+m^2)}\left(w_i^j-mu_i^j\right)-\frac{w_i^j}{K}$$

-----(35)

$$\left(\frac{\theta_i^{j+1}-\theta_i^j}{\Delta t}\right)-4\left(\frac{\theta_{i+1}^j-\theta_i^j}{\Delta y}\right)=\frac{4}{\Pr}\left(\frac{\theta_{i+1}^j-2\theta_i^j+\theta_{i-1}^j}{(\Delta y)^2}\right)$$---(36)

$$\left(\frac{\phi_i^{j+1}-\phi_i^j}{\Delta t}\right)-4\left(\frac{\phi_{i+1}^j-\phi_i^j}{\Delta y}\right)=\frac{4}{Sc}\left(\frac{\phi_{i+1}^j-2\phi_i^j+\phi_{i-1}^j}{(\Delta y)^2}\right)$$----(37)

Where the indices i also j denote to y as well as t respectively. The initial also boundary conditions (30) yield

$$\left.\begin{aligned}&u_i^0=0,\ w_i^0=0,\ \theta_i^0=0,\ \phi_i^0=0\ \ for\ all\ i,\\&u_i^j=0,\ \ w_i^j=0,\ \ \theta_i^j=e^{i\omega t},\ \phi_i^j=e^{i\omega t}\ \ at\ i=0\\&\&\ u_M^j\to 0,\ w_M^j\to 0,\ \theta_M^j\to 0,\ \phi_M^j\to 0\end{aligned}\right\}$$

------(38)

Thus the standards of *u*, *w*, "θ and ϕ" at "grid" point $t = 0$ are recognised; therefore the hotness field consumes been solved at time $t_{i+1}=t_i+\Delta t$ expending the identified standards of the previous time $t=t_i$ for all $i=1, 2, \ldots\ldots, N-1$. Then the velocity field is estimated by the previously recognised values of hotness and concentration fields achieved at $t_{i+1}=t_i+\Delta t$. These procedures are frequent till the necessary answer of *u*, *w*, θ and ϕ is increased at convergence standards:

$$abs\left|(u,\ w,\ \theta,\ \phi)_{exact}-(u,\ w,\ \theta,\ \phi)_{numerical}\right|<10^{-3}$$ ---(39)

IV. AUTHENTICATION OF "NUMERICAL_RESULTS":

In command to evaluate the scope of the final optimized technique, the authors associated the consequences through quantitative data used to detect the presence of frequency Parameter and Schmidt number. The current results are monitored with the available data of Sharma and Chowder [21], without Jeffrey's fluid and inclination of angle. These results in table 1 show some of the most complex computational and numerical methods. Therefore, you can use custom code and appropriate security to troubleshoot issues related to this document.

Table-1.: Sh is the Rate of figure transmission (Sherwood_number) results achieved in the current study, also $C(t)$ is the rate of mass transfer results gotten by Sharma as well as Chaudhary [28].

	$C(t)$ (Analytical results of Sharma and Chaudhary [28])			Sh (Present Numerical results)		
$\omega\downarrow$ $Sc\rightarrow$	0.22	0.30	0.78	0.22	0.30	0.78
0.0	0.2200	0.3000	0.7800	0.2200000000	0.3000000000	0.7800000000
0.2	0.0800	0.1200	0.3800	0.0799521658	0.1196448015	0.3793887414
0.4	-0.1700	-0.2100	-0.4100	-0.1699852164	-0.2093156348	-0.4082201332
0.6	-0.2700	-0.3500	-0.8100	-0.2666651428	-0.34931174524	-0.8073004784
0.8	-0.0800	-0.1200	0.3900	-0.0799962154	-0.11855470221	0.3893004523
1.0	0.2100	0.2600	0.4400	0.2099931524	0.25422185223	0.4393301666

V. RESULTS AND DISCUSSIONS:

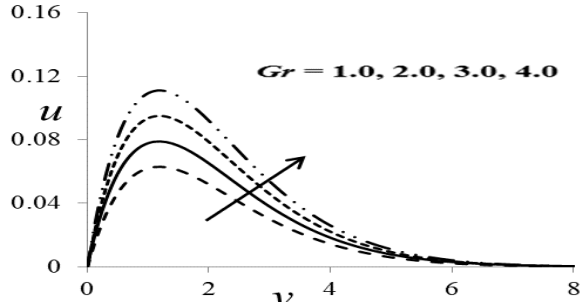

Fig_3. Effect of *Gr* on *u*

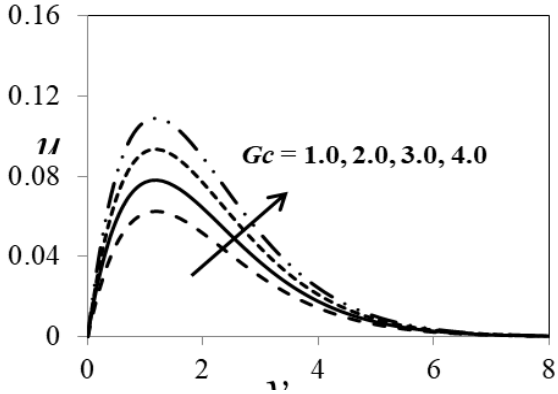

Fig._4. Effect of *Gc* on *u*

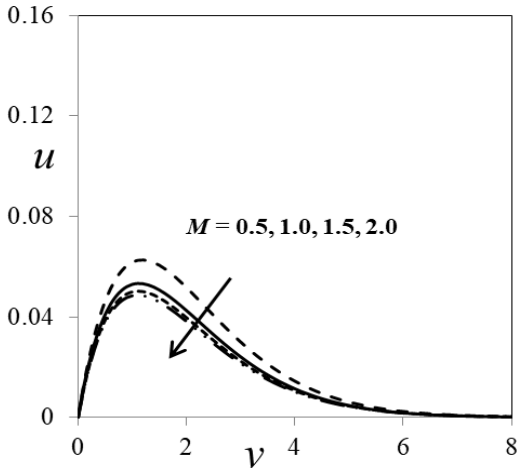

Figu/5. "Effect of *M*"

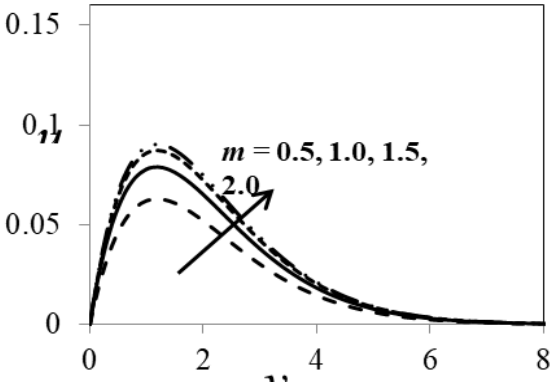

Fig:/6. "Effect" of *m* on

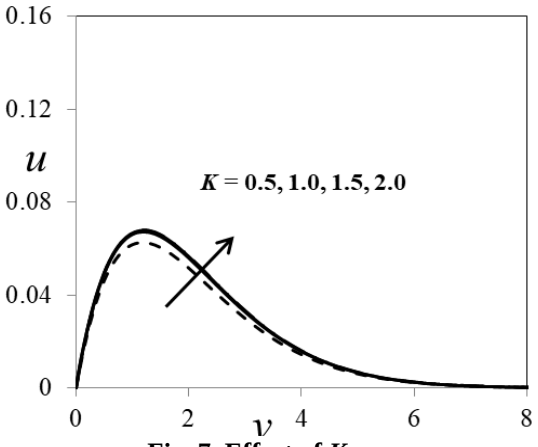

Fig. 7. Effect of *K* on *u*

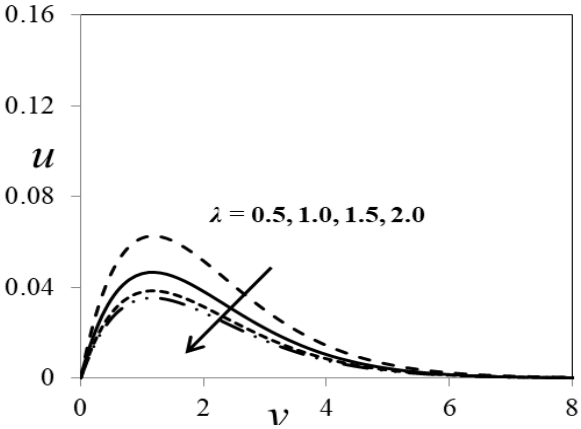

Fig. 8. Effect of *λ* on *u*

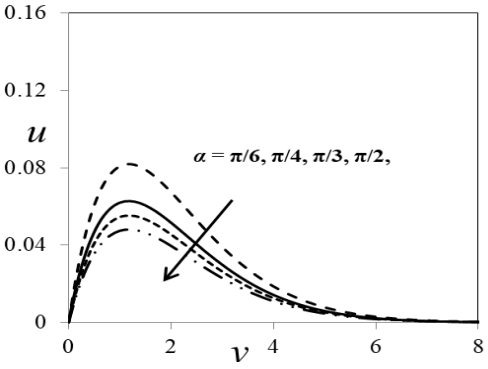

Fig. 9. Result of *α* on *u*

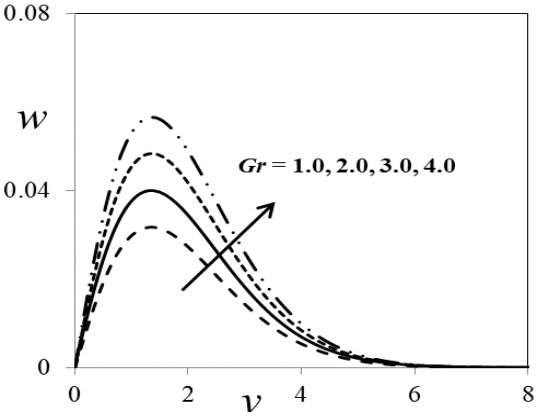

Fig. 10. Outcome of *Gr* on *w*

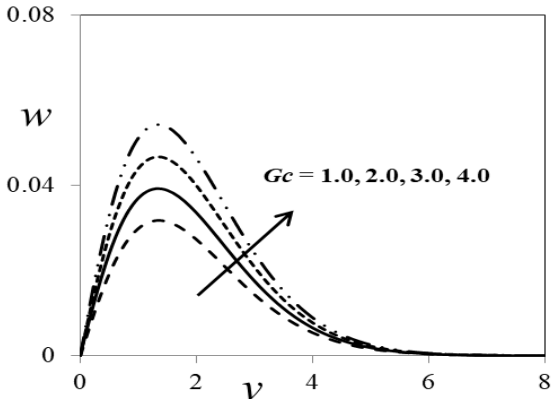

Fig. 11. Result of *Gc* on *w*

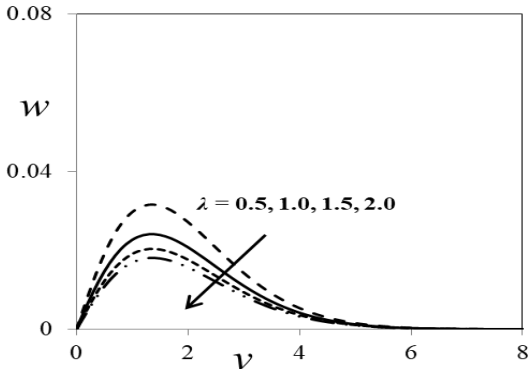

Fig. 15. Conclusion of λ on *w*

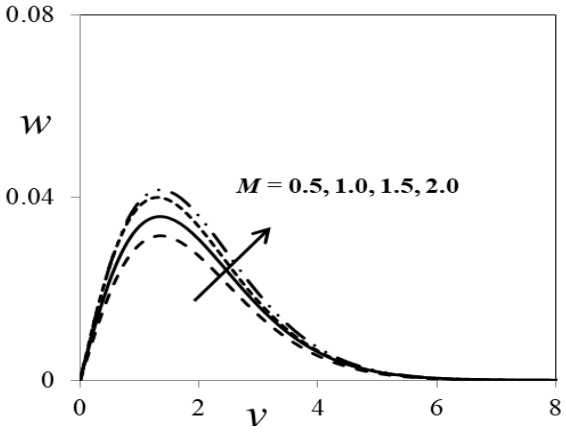

Fig. 12. Outcome of *M* on *w*

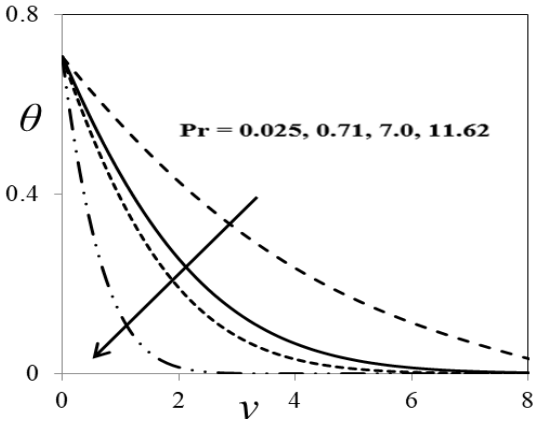

Fig. 16. Result of Pr on θ

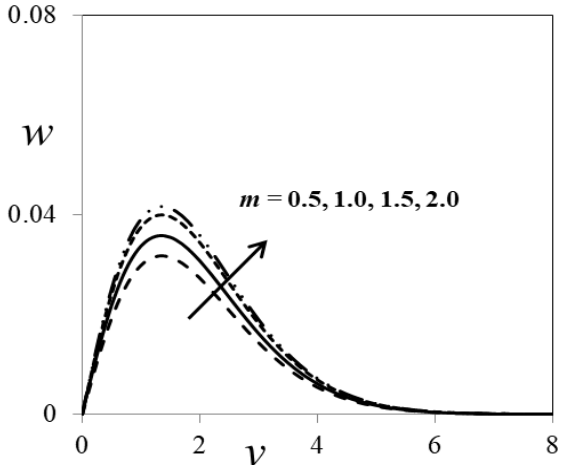

Fig. 13. Effect of *m* on *w*

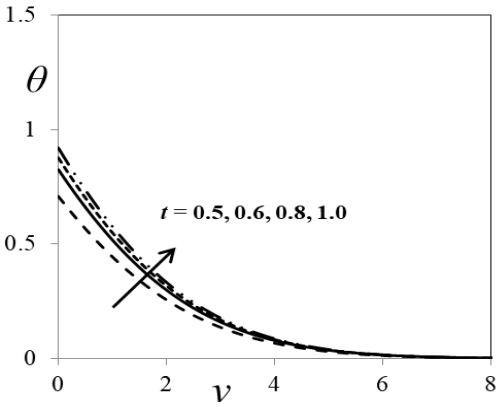

Fig. 17. Influence of *t* on θ

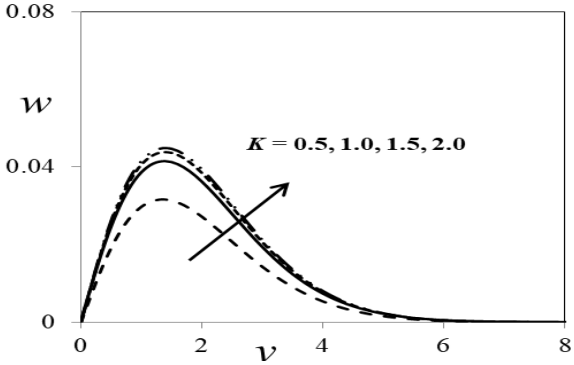

Fig. 14. Effect of *K* on *w*

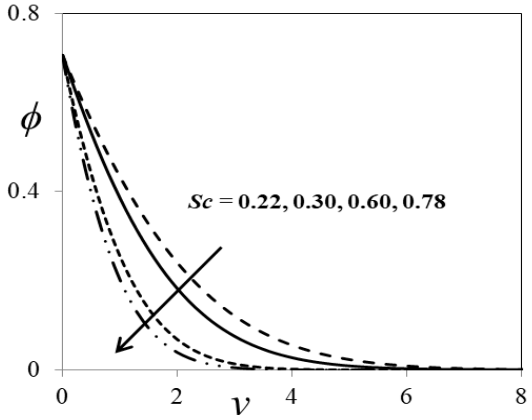

Fig. 18. Result of *Sc* on ϕ

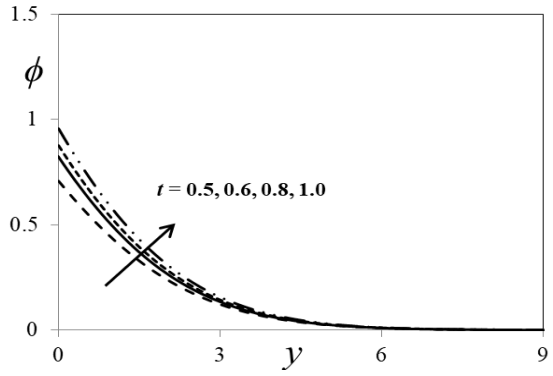

Fig. 19. Conclusion of t on ϕ

Equations (26), (27), (28), and (29) are the same and are solved numerically using constraints (30). The graphical portrayal of numerical outcomes is appeared in Figures (3) through (19) to demonstrate the impact of a few numbers on limit level stream. In this examination, we explore the impacts of different material parameters, for example, Grashof number for warmth move, Grashof number for mass exchange, attractive field parameter, Hall parameter, Jeffrey's liquid penetrability, and liquid parameters, and their particular edge of intrigue parameters To decide the impact. Conveyances of speed, temperature, additionally focus. The numerical aftereffects of the skin-grinding coefficient, heat rate, and mass exchange coefficients, communicated as Nusselt number or Sherwood number, are introduced in table structure. Major velocity, secondary velocity, temperature in addition to numerical calculations attentiveness, selected standards mercury ("Pr=0.025"), "air_was 25^oC" and atmospheric compression (Pr = 0.71), water (Pr = 7.00) & water at "$4°C$ (Pr = 11.40)". emphasize the value of the results obtained in this study, *Sc* values were hydrogen (*Sc* = 0.22), helium (*Sc* = 0.30), water vapour (*Sc* = 0.60) and ammonia (*Sc* = 0.78). For physical meaning, numerical discussions are disputed and at t = 1.0, $\omega t = \pi / 2$ to obtain stable values for velocity, temperature and focus area. To find a solution to this problem, infinite vertical unlimited plates are introduced into the stream. This solves a limited problem. However, in the image, the value of y varies from 0 to 8. The velocity, temperature and concentration profiles tend to be zero at y_{max} = 8. They tend to be 8. This applies to any value and this study takes a long time.

The temperature and concentrations of the flow are combined at the primary V using the Grashof warmth transmission amount, also the Grash_of mass transmission number is shown in equation (26). The influence of Grash/of numbers on warmth and mass transfer on the primary V profile is shown in the Figure_3 & 4, correspondingly. Grash_of numbers for heat transfer numbers relate to the relative guidance of thermal decomposition on the dynamics of a viscous fluid in a border layer. As expected, an increase in the main speed was observed after an increase in thermal power. If *Gr* increases, the maximum velocity of the fundamental velocity near the resonator plate increases rapidly, and then gradually decreases at a free flow velocity. Grashof mass transfer determines the relationship between species richness and fluid dynamics. True to form, as species engaging quality expands, the liquid speed increments and the pinnacle turns out to be progressively perceptible. The profile of the essential speed arrives at a critical most extreme close to the plate and hence exactly diminishes to gauge the estimation of the free stream. It ought to be noticed that the essential speed increments with the expansion in the mass trade of Grashof number for mass exchange. Figs. 5 and 12 demonstrate the impact of attractive field parameters on the essential and auxiliary speeds, individually. As can be seen from these figures, with an expansion in M, both the essential and auxiliary speeds decline. That is, essential or auxiliary liquids are deferred because of the utilization of a flat attractive field. This marvel is obviously reliable with the way that the Lorentz power is because of the association of the attractive field and the liquid speed contingent upon the smooth movement. The impact of Grash.of numbers for warmth and mass exchange numbers on the auxiliary speed dispersion is appeared in the Figure.10 &11. With expanding warmth move and mass, this auxiliary speed part additionally increments. The impact of the Hall parameter m on the profile of the essential and auxiliary are appeared in the Figs. 6 and 13. From these figures, it is seen that the essential and auxiliary speeds increment the Hall parameter. This is on the grounds that the Hall current as a rule diminishes the Lorentz power. This implies while home will in general increment its segment of liquid speed. Fig. 18 demonstrates the centralization of different gases on the y-hub, for example, HYDROGEN_(Sc = 0.22), helium_(Sc = 0.30), water_vapor (Sc = 0.60), and smelling salts (Sc = 0.780). It was accounted for that the impact of expanding the Schmitt number (Sc) diminishes the fixation. This is reliable with the way that an expansion in Sc implies a decline in atomic dispersion (D), which prompts a diminishing in the centralization of the limit layer. Thusly, for lower estimations of Sc, the convergence of the material is more noteworthy, and for huge estimations of Sc, the centralization of the material is lower. Also, it was noticed that the thickness of the fixation limit layer expanded fundamentally with an expanding recurrence close to the limit, however the contrary pattern was found a long way from the plate. Bends on the graph. Figs. 7 and 14 demonstrate the impact of the Permeability parameter (K) on the essential and auxiliary velocities, individually. As appeared in outlines 7 and 14, as these Permeability parameters increment, the two speeds in the x' and z' bearings increment. Fig. 16 demonstrates the impact of Pr (Prandtl) numbers on the temperature profile. The proportion of thickness to warmth is Prandtl number Pr. From this figure, it is seen that the temperature of the liquid reductions with expanding estimation of the Prandtl number. Physically, this might be because of the way that liquid with a huge Prandtl number has a higher thickness, which makes the fluid thicker and along these lines backs off.

Figs. 17 and 19 demonstrate the impact of time on temperature and focus profiles. It very well may be seen from these assumes that θ and ϕ increment with t. This implies the temperature and convergence of the liquid quicken after some time on the limit layer.

The impact of the Jeffrey parameter (λ) on the liquid speed profile in the x' (essential speed) and z' (auxiliary speed) headings has graphically appeared in Figs. 8 and 15, separately. It very well may be seen from these assumes that to expand the estimation of both Jeffrey parameter, the liquid stream rate (essential speed and optional speed) diminishes in the limit layer district. The Jeffrey parameter estimates the yield quality, and when it turns out to be enormous, the liquid carries on like a Newtonian liquid. The subsequent increment in weight causes an adjustment impact. The impact of the point of a tendency to the vertical on the speed has appeared in Fig. 9. From this figure, we see that the speed diminishes with expanding edge of tendency because of the way that the edge of tendency builds the impact of lightness because of an abatement in warmth age by the coefficient cosα. Accordingly, the power following up on the liquid abatements because of a decline in the speed profiles. The impact of Gr, Gc, M, m, K, Pr, Sc, α and λ on the skin grinding coefficient (Cf1) as the fundamental speed profile is examined in Tables 2 and 3. From this table it tends to be seen that the coefficient of coefficient increments with expanding Gr esteem, Gc, m, K and the contrary impact was seen with expanding M, Pr, Sc, α, λ. The impacts of Gr, Gc, M, m, K, Pr, Sc, α, and λ on the skin grating coefficient (Cf2) because of the optional speed profiles are talked about in Tables 4 and 5. From this table, the skin rubbing coefficient increments with expanding Gr esteem, Gc, M, m, K, and the contrary impact were seen with expanding Pr, Sc, α, λ. The impact of Pr and t on the warmth move coefficient (Nu) because of the temperature profiles is examined in Table 6. It very well may be seen from this table the warmth move coefficient increments with expanding t and diminishes with expanding Pr. The impact of Sc and t on the mass exchange coefficient or Sherwood number (Sh) as the focus profiles is talked about in Table 7. It tends to be seen from this table the mass exchange coefficient increments with expanding t, diminishing with expanding Sc.

Table_2.: Mathematical_values of "Skin/friction" coeff (Cf_1) due to PV profiles for dissimilar standards of *Gr*, *Gc*, *M*, *K* and *m*

'Gr	*'Gc*	*'M*	*'K*	*m*	Cf_1
2.0	2.0	0.5	0.5	0.5	1.2655489215
4.0	2.0	0.5	0.5	0.5	1.4200185246
2.0	4.0	0.5	0.5	0.5	1.4423665842
2.0	2.0	1.0	0.5	0.5	1.1500247783
2.0	2.0	0.5	1.0	0.5	1.3065521866
2.0	2.0	0.5	0.5	1.0	1.3046625778

Table_3.: Numerical(NL) standards of Skin_friction coefficient (Cf_1) "due to PV" profiles for dissimilar standards of *λ*, *α*, Pr and *Sc*

λ	*α*	Pr	*Sc*	Cf_1
0.5	45°	0.71	0.22	1.2655489215
1.0	45°	0.71	0.22	1.1620047778
0.5	90°	0.71	0.22	1.1752284157
0.5	45°	7.00	0.22	1.1966023347
0.5	45°	0.71	0.30	1.1833244756

Table_4.: Numerical values of Skin-friction coefficient (Cf_2) due to secondary velocity profiles for different values of *Gr*, *Gc*, *M*, *K* and *m*

Gr	*Gc*	*M*	*K*	*m*	Cf_2
2.0	2.0	0.5	0.5	0.5	0.4855212659
4.0	2.0	0.5	0.5	0.5	0.6822014785
2.0	4.0	0.5	0.5	0.5	0.7022688124
2.0	2.0	1.0	0.5	0.5	0.3153000069
2.0	2.0	0.5	1.0	0.5	0.5326615466
2.0	2.0	0.5	0.5	1.0	0.5266044746

Table-5.: Mathematical values of Skin_friction coefficient (Cf_2) due to secondary_velocity profiles for dissimilar "values" of *λ*, "Pr" and "*Sc*"

λ	Pr	*Sc*	Cf_2
0.5	0.71	0.22	0.4855212659
1.0	0.71	0.22	0.3215565948
0.5	7.00	0.22	0.3052221478
0.5	0.71	0.30	0.3166980024

Table-6.: Arithmetical standards of rate of heat transfer coefficient (*Nu*) due to temperature profiles for different values of Pr and *t*

Pr	*t*	*Nu*
0.71	1.0	0.1699230154
7.00	1.0	0.1132265466
0.71	2.0	0.2544102134

Table-7.: Numerical values of rate of mass transfer coefficient (*Sh*) due to "concentration" profiles for different values of *Sc* and *t*

"Sc"	*t*	Cf_2
0.22/	1.00	0.1622955016
0.30/	1.00	0.1245520113
0.22/	2.00	0.2542201348

VI. CONCLUSIONS

In this research work, the combined actions of hall current and magnetic fields on laminar, viscous, and electric currents directed by Jeffrey's fluid_flow to the forefront of H and m transfer. The incomplete differential eq of the principal linear repressors are solved using the finite difference method. The following assumptions are "drawn" from this research work:

i. Due to the Lorentz force, the primary and secondary profiles decrease with increasing magnetic field, and the opposite effect is experiential in the P and "secondary" profiles in presence of hall current parameter.

ii. It has been found that Grashof numbers which increase heat transfer and mass increase the effect of buoyancy and heat concentration, thus increasing P and secondary_velocities.

iii. "With_the_increasing" Schmidt number, the distribution of concentration decreases at all points. This means that the most common material has a significant delay in the circulation of the flow field concentration.

iv. Intravenous Number Prandtl reduces the flow_field temperature at very points. The advanced the Prandtl number, the lower the flow field temp decreases.

v. Against the Decisions made in the matter of a particular problem compared to those published and well received.

Nomenclature:

List of variables:

T'_∞	Fluid temperature "far away from the" plate (K)
T'_w	Temperature of the plate (K)
Gr	Grash_of number for heat transfer
m	Hall parameter
C'_w	Concentration of the fluid at the wall $(Kg\,m^{-3})$
g	Acceleration due to gravity $(m\,s^{-2})$
D	Chemical molecular diffusivity $(m^2\,s^{-1})$
D_T	Coefficient of chemical thermal diffusivity, $M^1L^{-1}T^{-1}K^{-1}$
$\overline{B}$	Magnetic Induction Vector
C'_∞	Concentration in the fluid far away From the plate $(Kg\,m^{-3})$
C'	Dimensionless species concentration of the fluid
$\overline{J}$	Electric current density vector
$\overline{E}$	Electric field
e	Electron charge, $Coloumi$
p_e	Electron pressure $(N\,m^{-2})$
Gc	Grashof number for mass transfer
M	Hartmann number or Magnetic field parameter

B_o "Intensity of the applied magnetic _field" $(A\,m^{-1})$

K Permeability of the porous medium

Pr Prandtl number

V_o Reference velocity $(m\,s^{-1})$

Sc Schmidt number

Cf_1 Skin-friction due to velocity (u) (N/m^2)

Cf_2 Skin-friction due to velocity (w) (N/m^2)

C_p Specific heat at constant pressure $(J\,Kg^{-1}K)$

T' "Temperature" of the_fluid (K)

t Time (s)

w Velocity component in z' −direction $(m\,s^{-1})$

u Velocity component in x' −direction $(m\,s^{-1})$

$\vec{V}$ Velocity vector

Nu Rate of heat transfer coefficient (or) Nusselt number

Sh Rate of mass transfer coefficient (or) Sherwood number

Greek symbols:

λ Jeffrey fluid parameter

α Angle of inclination parameter *(degrees)*

κ Thermal conductivity, W/mK

ρ Density of the fluid (kg/m^{-3})

Ω Angular frequency *(Hertz)*

β Coefficient of Volume expansion (K^{-1})

θ Dimensionless Temperature (K)

σ Electrical conductivity, $(\Omega^{-1}m^{-1})$

τ_e Electron collision time (s)

ω_e Electron frequency *(Hertz)*

ω Frequency parameter

τ_i Ion collision time (s)

ω_i Ion frequency *(Hertz)*

ν Kinematic Viscosity (m^2s^{-1})

n_e Number of electron density

ωt Phase Angle *(radians)*

τ'_w Shear stress (N/m^2)

β^* Volumetric Coefficient of expansion with Concentration $(m^3\,Kg^{-1})$

Superscript:

$'$ Dimensionless properties

Subscripts:

w "Conditions on the wall"

∞ "Free stream conditions"

p Plate

REFERENCES:

1. T. G. Cowling, Magnetohydrodynamics, Interscience Publishers, New York (1957).
2. M. C. Raju, S. V. K. Varma, N. Ananad Reddy, Hall-current effects on unsteady magnetohydrodynamics flow between stretching sheet and an oscillating porous upper parallel plate with constant suction, Thermal Sci., 15 (2) (2011), pp. 45-48.
3. M. Veera Krishna., M. Gangadhar Reddy, MHD Free Convective Boundary Layer Flow through Porous medium Past a Moving Vertical Plate with Heat Source and Chemical Reaction, Mater. Today Proc., 5 (2018), pp. 91-98, 10.1016/j.matpr.2017.11.058.
4. B. Prabhakar Reddy, J. Anand Rao, Radiation and thermal diffusion effects on an unsteady MHD free convection mass-transfer flow past an infinite vertical porous plate with the hall current and a heat source, J. Eng. Phys. Thermophys., 84 (6) (2011), pp. 1369-1378.
5. A. M. Rashad, S. Abbasbandy, A. J. Chamkha, Non-Darcy Natural Convection From a Vertical Cylinder Embedded in a Thermally Stratified and Nanofluid-Saturated Porous Media, J. Heat Transf., 136 (2) (2014), Article 022503, 10.1115/1.4025559.
6. M. M. Rashidi, S. Abelman, N. Freidooni Mehr, Entropy generation in steady MHD flow due to a rotating porous disk in a nanofluid, Int. J. Heat Mass Transf., 62 (2013), pp. 515-525, 10.1016/j.ijheatmasstransfer.2013.03.004.
7. T. Watanabe, I. Pop, Hall effects on magnetohydrodynamic boundary layer flow over a continuous moving flat plate, Acta Mech., 108 (1) (1995), pp. 35-47.
8. B. K. Sharma, A. K. Jha, R. C. Chaudhary, Hall effect on MHD mixed convective flow of a viscous incompressible fluid past a vertical porous plate immersed in porous medium with heat source/sink, Rom. J. Phys., 52 (5–7) (2007), pp. 487-503.
9. E. Sawaya, N. Ghaddar, F. Chaaban, Evaluation of the Hall parameter of electrolyte solutions in thermo-syphonic MHD flow, Int. J. Eng. Sci., 31 (7) (1993), pp. 1073-1091.
10. R. Bhargava, H. S. Takhar, Effect of Hall currents on the MHD flow and heat transfer of a second order fluid between two parallel porous plates, J. MHD, Plasma Space Res., 10 (2001), pp. 73-87.
11. K. Maqbool, A. B. Mann, M. H. Tiwana, Unsteady MHD convective flow of a Jeffery fluid embedded in a porous medium with ramped wall velocity and temperature, Alexandria Eng. J., Vol. 57, Issue 2, pp. 1071-1078, 2018.
12. F. M. Abbasi, S. A. Shehzad, A. Alsaedi, T. Hayat, Simultaneous effects of convective heat and mass conditions in magnetohydrodynamic three-dimensional flow of Jeffrey fluid with thermophoresis, J. Aerosp. Eng., 29 (4) (2016), p. 04016013.
13. F. M. Abbasi, S. A. Shehzad, T. Hayat, M. S. Alhuthali, Mixed convection flow of jeffrey nanofluid with thermal radiation and double stratification, J. Hydrodyn. Ser. B, 28 (5) (2016), pp. 840-849.
14. I. Khan, A note on exact solutions for the unsteady free convection flow of a Jeffrey fluid, Zeitschrift fur Naturforschung A, 70 (6) (2015), pp. 272-284.
15. K. Vajravelu, S. Sreenadh, P. Lakshminarayana, G. Sucharitha, The effect of heat transfer on the nonlinear peristaltic transport of a Jeffery fluid through a finite vertical porous channel, Int. J. Biomath., 9 (2008), 1650023, 24 pages.
16. P. Lakshminarayana, S. Sreenadh, G. Sucharitha, K. Nandgopal, Effect of slip and heat transfer on peristaltic transport of a Jeffrey fluid in a vertical asymmetric porous channel, Adv. Appl. Sci. Res., 6 (2) (2015), pp. 107-118.

17. K. Vajravelu, S. Sreenadh, P. Lakshminarayana, The influence of heat transfer on peristaltic transport of a Jeffrey fluid in a vertical porous stratum, Commun. Nonlinear Sci. Numer. Simul., 16 (8) (2011), pp. 3107-3125.
18. K. Vajravelu, S. Sreenadh, G. Sucharitha, P. Lakshminarayana, Peristaltic transport of a conducting Jeffrey fluid in an inclined asymmetric channel, Int. J. Biomath., 7 (6) (2014), 1450064 (25 pages).
19. A. R. Butt, M. Abdullah, N. Raza, M. A. Imran, Influence of non-integer order parameter and Hartmann number on the heat and mass transfer flow of a Jeffery fluid over an oscillating vertical plate via Caputo-Fabrizio time fractional derivatives, The Euro. Phy. J. Plus, Vol. 132, pp. 414, 2017.
20. Maria Imtiaz,Tasawar Hayat, Ahmed Alsaedi, MHD Convective Flow of Jeffrey Fluid Due to a Curved Stretching Surface with Homogeneous-Heterogeneous Reactions, PLoS ONE J., Vol. 11, Issue 9, e0161641. https://doi.org/10.1371/journal.pone.0161641.
21. B. K. Sharma, R. C. Chaudhary, Hydromagnetic Unsteady Mixed Convection And Mass Transfer Flow Past A Vertical Porous Plate Immersed In A Porous Medium With Hall Effect, Eng. Trans., 56, 1, 3-23 (2008).
22. P. Sturdza, An Aerodynamic design method for supersonic natural laminar flow aircraft Ph. D. thesis. California, USA: Dept. Aeronautics and Astronautics, Stanford University (2003).